PAPER

Eigen Analysis of Space Embedded Equation in Moment Vector Space for Multi-dimensional Chaotic Systems

Hideki SATOH[†], *Member*

SUMMARY Multi-dimensional chaotic systems were reduced to low-dimensional space embedded equations (SEEs), and their macroscopic and statistical properties were investigated using eigen analysis of the moment vector equation (MVE) of the SEE. First, the state space of the target system was discretized into a finite discrete space. Next, an embedding from the discrete space to a low-dimensional discrete space was defined. The SEE of the target system was derived using the embedding. Finally, eigen analysis was applied to the MVE of the SEE to derive the properties of the target system. The geometric increase in the dimension of the MVE with the dimension of the target system was avoided by using the SEE. The pdfs of arbitrary elements in the target nonlinear system were derived without a reduction in accuracy due to dimension reduction. Moreover, since the dynamics of the system were expressed by the eigenvalues of the MVE, it was possible to identify multiple steady states that cannot be done using numerical simulation. This approach can thus be used to analyze the macroscopic and statistical properties of multi-dimensional chaotic systems.

key words: *chaos, GCM, MVE, nonlinear, dimension reduction*

1. Introduction

There is a need to address high-dimensional nonlinear systems in various fields, such as pattern recognition, clustering, control, and analysis. Solving nonlinear high-dimensional problems requires reducing the dimension of the state space. However, dimension reduction for arbitrary high-dimensional nonlinear systems is a very difficult problem.

Various methods have thus been developed for solving restricted types of problems. Nonlinear principal component analysis (PCA), which uses nonlinear axes [1], [2], can extract nonlinear relationships in high-dimensional data and express the data in a low-dimensional space more effectively than linear PCA. A basis function is important for effectively expressing high-dimensional data in a low-dimensional space. A radial basis function has attracted much interest because it can be smoothly modified by adjusting its parameters [3]. In the Laplacian approach, nearby samples are connected on the basis of the state space geometry using the graph Laplacian, and basis elements are set to the eigen vectors of the Laplacian [4], [5].

However, the low-dimensional model is often incomplete because the data do not always cover all the dynamics of the target system. For example, if the target system has multiple steady states and some steady states rarely appear, the data obtained from the target system may not contain all the steady states.

This problem can be avoided by using analytical model reduction. The high-dimensional state is reduced analytically by extracting the phase dynamics of the state to analyze various oscillations of the state [6]. Center-manifold reduction can be used for analyzing the change in the state in the neighborhood of a bifurcation point [7], which is difficult to do using numerical analysis. While perturbation analysis and asymptotic analysis, which are widely used and theoretically supported, are effective for solving various nonlinear problems [8], [9], they cannot always be applied to arbitrary systems. Moreover, approximate solutions obtained with these methods are rather complex, so they cannot easily be used to construct everyday systems.

Eigen analysis of the Frobenius-Perron operator is used to derive the probability density function (pdf) representing the macroscopic and statistical properties of the system [10], [11]. Application of the Galerkin approximation to the Frobenius-Perron operator enables the pdfs of nonlinear systems to be derived with high accuracy. However, the dimension of the coefficient vector used for the Galerkin approximation increases geometrically with the dimension for a given accuracy. This "curse of dimensionality" problem prevents using this method for analyzing a high-dimensional nonlinear system.

Eigen analysis of the moment vector equation (MVE) is used to investigate the macroscopic and statistical properties of nonlinear systems [12], [13]. However, it is also affected by the curse of dimensionality. A many-body system can be expressed using a Boltzmann equation [14] or a nonlinear Fokker-Planck equation [15] if the elements in the system are identical and indistinguishable. Although the MVE has been expanded for use in analyzing a many-body system [13], it is still difficult to use the MVE for a high-dimensional system if it is not expressed as a many-body system.

The MVE of a space embedded equation (SEE) presented in this paper is applied to this problem. The SEE can express an arbitrary multi-dimensional target system as a low-dimensional equation. The pdfs of arbitrary elements in the target nonlinear system are derived without a reduction in accuracy due to dimen-

Manuscript received June 27, 2012.
Final manuscript received September 20, 2012.

[†]The author is with the Future University Hakodate, Hakodate-shi, 041-8655 Japan.

sion reduction. Moreover, the dynamics of the system are expressed by the eigenvalues of the MVE, making it possible to identify multiple steady states that cannot be identified using numerical simulation.

In Sect. 2, analysis using the MVE is summarized. Section 3 describes the method for expressing a multi-dimensional system as a low-dimensional SEE. In Sect. 4, it is shown that the MVE of the SEE and its eigen analysis can be used to derive the properties of multi-dimensional chaotic systems. The key points are summarized and areas for future work are mentioned in Sect. 5.

2. Analysis of Nonlinear System Using Moment Vector Equation

2.1 Moment Vector Equation for Nonlinear System

Consider the problem of deriving the dynamics of a nonlinear system using an equation of the system given in advance. Although numerical simulation is powerful, all the dynamics of the system cannot always be identified [13]. The moment vector equation (MVE) was developed to identify thy dynamics that cannot be identified using numerical simulation [12], [13].

Consider the following multi-dimensional discrete-time nonlinear system:

$$\boldsymbol{s}_{t+1} = \boldsymbol{f}(\boldsymbol{s}_t), \tag{1}$$

where $\boldsymbol{s}_t \stackrel{\text{def}}{=} (s_{1;t}, \cdots, s_{d_\mathrm{s};t})^\mathrm{T} \in \mathcal{D}_\mathbf{s}$ is the state of dimension d_s, $\boldsymbol{f}(\cdot) \stackrel{\text{def}}{=} (f_1(\cdot), \cdots, f_{d_\mathrm{s}}(\cdot))^\mathrm{T}$ is a deterministic or stochastic function, subscript t denotes a discrete time, $\mathcal{D}_\mathbf{s} \stackrel{\text{def}}{=} \{\boldsymbol{s}_t | s_{\min d} < s_{d;t} < s_{\max d}, 1 \le d \le d_\mathrm{s}\}$ is the domain of definition, and superscript T denotes a transposition.

Let $\{\psi_i(\cdot)\}$ be an orthonormal basis and $\psi_0(\cdot)$ be constant ψ_0 as defined in Appendix A. To derive the MVE for the nonlinear system in Eq. (1), we introduce the following assumption with respect to Eq. (1).

Assumption 1: We can expand $E[\psi_i(\boldsymbol{s}_{t+1})|\boldsymbol{s}_t]$ in a Fourier series:

$$E[\psi_i(\boldsymbol{s}_{t+1})|\boldsymbol{s}_t] = \sum_{j=0}^{N} a_{ij}\psi_j(\boldsymbol{s}_t) + \varepsilon_i(\boldsymbol{s}_t), \tag{2}$$

where $E[\cdot]$ is the mathematical expectation, $\varepsilon_i(\boldsymbol{s}_t)$ is the residual, and N is the degree of expansion. □

Using Eq. (2), we can expand $E[\psi_i(\boldsymbol{s}_{t+1})]$:

$$\begin{aligned} E[\psi_i(\boldsymbol{s}_{t+1})] &= \int p(\boldsymbol{s}_t)(\sum_{j=0}^{N} a_{ij}\psi_j(\boldsymbol{s}_t) + \varepsilon_i(\boldsymbol{s}_t))\mathrm{d}\boldsymbol{s}_t \\ &= \sum_{j=0}^{N} a_{ij}E[\psi_j(\boldsymbol{s}_t)] + E[\varepsilon_i(\boldsymbol{s}_t)], \end{aligned} \tag{3}$$

where $p(\cdot)$ denotes a probability density function. When Eq. (1) is deterministic, a_{ij} is derived from Eq. (A·2) as

$$a_{ij} = \int_{\mathcal{D}_\mathbf{s}} \psi_i(\boldsymbol{f}(\boldsymbol{s}))\psi_j^*(\boldsymbol{s})\mathrm{d}\boldsymbol{s}, \tag{4}$$

where superscript $*$ denotes a complex conjugate. If we assume that $E[\varepsilon_i(\boldsymbol{s}_t)] = 0$, Eq. (3) can be expressed as

$$\boldsymbol{\rho}_{t+1} = A\boldsymbol{\rho}_t, \tag{5}$$

where $\boldsymbol{\psi}(\boldsymbol{s}_t) \stackrel{\text{def}}{=} (\psi_0(\boldsymbol{s}_t), \cdots, \psi_N(\boldsymbol{s}_t))^\mathrm{T}$, $\boldsymbol{\rho}_t \stackrel{\text{def}}{=} E[\boldsymbol{\psi}(\boldsymbol{s}_t)]$ is referred to as the moment vector, and A is the $(N+1)\times(N+1)$ matrix defined by

$$A \stackrel{\text{def}}{=} [a_{ij} | 0 \le i \le N, 0 \le j \le N].$$

Equation (5) is referred to as the MVE.

2.2 Infinite-time Average of Moment Vector Corresponding to Multiple Equilibrium Points

Let $\langle\boldsymbol{\rho}_t\rangle$ be the infinite-time average of $\boldsymbol{\rho}_t$ defined by

$$\langle\boldsymbol{\rho}_t\rangle \stackrel{\text{def}}{=} \lim_{T\to\infty} T^{-1}\sum_{\tau=0}^{T-1}\boldsymbol{\rho}_{t+\tau}.$$

The following assumption is introduced for convenience of analysis to derive the infinite-time average of moment vector $\boldsymbol{\rho}_t$.

Assumption 2: $\boldsymbol{\rho}_t$ does not diverge for $t \to \infty$. □

Let λ_i be the ith eigenvalue of matrix A in Eq. (5), $\boldsymbol{e}_i$ be the ith eigenvector of matrix A $(0 \le i \le N)$, and λ_i and $\boldsymbol{e}_i$ be arranged by the value of λ_i so that

(a) $\lambda_0 = 1$ and $e_{00} \neq 0$,
(b) $\lambda_i = 1$ and $e_{i0} = 0$ for $0 < i \le i_1$,
(c) $\|\lambda_i\| = 1$, $\lambda_i \neq 1$, and $e_{i0} = 0$ for $i_1 < i \le i_2$,
(d) $\|\lambda_i\| < 1$ and $e_{i0} = 0$ for $i_2 < i \le N$.

Here, $\|\lambda_i\| \le 1$ holds for $\forall i$ from Assumption 2, and $\rho_{0;t}$ is constant because $\psi_0(\cdot)$ is constant from the definition of $\{\psi_i(\cdot)\}$. Thus, there is at least one eigenvalue that is equal to one, $e_{00} \neq 0$ holds in (a), and $e_{i0} = 0$ holds in (b), (c), and (d).†

Because the MVE in Eq. (5) is linear, $\langle\boldsymbol{\rho}_\infty\rangle$ is equal to equilibrium point $\boldsymbol{\rho}_\mathrm{e}$ such that $\boldsymbol{\rho}_\mathrm{e} = A\boldsymbol{\rho}_\mathrm{e}$ even if $\boldsymbol{\rho}_t$ oscillates at $t = \infty$ [12]. Equilibrium point $\boldsymbol{\rho}_\mathrm{e}$ is expressed as a weighted sum of eigenvector $\boldsymbol{e}_i$ with $\lambda_i = 1$. Therefore, $\langle\boldsymbol{\rho}_\infty\rangle$ can be expressed as

$$\langle\boldsymbol{\rho}_\infty\rangle = (\psi_0/e_{00})\sum_{i=0}^{i_1} w_i\boldsymbol{e}_i. \tag{6}$$

The (ψ_0/e_{00}) is set so that the first element in $\langle\boldsymbol{\rho}_\infty\rangle$

†These properties are obvious from analysis using linear algebra.

equals ψ_0, and w_i is a given weight (w_0 is always set to unity). When there are multiple eigenvalues that take a value of 1, $\langle \boldsymbol{\rho}_\infty \rangle$ takes various values as determined by the $w_1, \cdots, w_{i_1}$ that are given corresponding to initial state $\boldsymbol{\rho}_0$.

The above equation contains information about the statistical properties not only when $\boldsymbol{s}_t$ converges but also when $\boldsymbol{s}_t$ oscillates. A method for deriving the probability density function (pdf) of $\boldsymbol{s}_t$ will be presented in the next section.

2.3 Probability Density Function Based on Moment Vector

The pdf of $\boldsymbol{s}_t$ of the nonlinear system in Eq. (1) in a steady state is derived using $\langle \boldsymbol{\rho}_\infty \rangle$.

Consider the Fourier series expansion of $\delta(\boldsymbol{s} - \hat{\boldsymbol{s}})$.

$$\delta(\boldsymbol{s} - \hat{\boldsymbol{s}}) \cong \sum_{i=0}^{N} \alpha_i \psi_i(\boldsymbol{s}), \tag{7}$$

where $\hat{\boldsymbol{s}}$ is a given constant vector, and Fourier coefficient α_i is derived using

$$\begin{aligned} \alpha_i &= \int \delta(\boldsymbol{s} - \hat{\boldsymbol{s}}) {\psi^*}_i(\boldsymbol{s}) \mathrm{d}\boldsymbol{s} \\ &= {\psi^*}_i(\hat{\boldsymbol{s}}). \end{aligned}$$

From this, we obtain

$$\delta(\boldsymbol{s} - \hat{\boldsymbol{s}}) \cong {\boldsymbol{\psi}^*}^{\mathrm{T}}(\hat{\boldsymbol{s}}) \boldsymbol{\psi}(\boldsymbol{s}). \tag{8}$$

Using this equation, we can approximate $\forall p(\boldsymbol{s})$ as

$$\begin{aligned} p(\boldsymbol{s}) &= \int p(\hat{\boldsymbol{s}}) \delta(\hat{\boldsymbol{s}} - \boldsymbol{s}) \mathrm{d}\hat{\boldsymbol{s}} \\ &\cong {\boldsymbol{\psi}^*}^{\mathrm{T}}(\boldsymbol{s}) E[\boldsymbol{\psi}(\boldsymbol{s})]. \end{aligned}$$

The pdf of $\boldsymbol{s}$ in a steady state is thus obtained by replacing $E[\boldsymbol{\psi}(\boldsymbol{s})]$ with $\langle \boldsymbol{\rho}_\infty \rangle$:

$$p(\boldsymbol{s}) = \langle \boldsymbol{\rho}_\infty \rangle^{\mathrm{T}} \boldsymbol{\psi}^*(\boldsymbol{s}). \tag{9}$$

Because this equation is an approximation, the $p(\boldsymbol{s})$ is not always greater than 0 due to the approximation error, although $\int p(\boldsymbol{s}) \mathrm{d}\boldsymbol{s} = 1$ always holds.

2.4 Structure Analysis Based on Eigenvalue and Eigenvector of Moment Vector Equation

A structure analysis based on eigen analysis is presented in this section. As shown in Eq. (9), the average pdf in a steady state is determined by $\langle \boldsymbol{\rho}_\infty \rangle$. The eigenvalues and eigenvectors of coefficient matrix A of the MVE in Eq. (5) determine the dynamics in the moment vector. The macroscopic structure and mechanism of the system are thus obtained by eigen analysis of the coefficient matrix.

Let λ_i be the ith eigenvalue of matrix A in Eq. (5) and $\boldsymbol{e}_i$ be the corresponding eigenvector. When the initial value of the moment vector is given by

$$\boldsymbol{\rho}_0 = \xi_0 \boldsymbol{e}_0 + \xi_1 \boldsymbol{e}_1 +, \cdots, +\xi_N \boldsymbol{e}_N,$$

$\boldsymbol{\rho}_t$ is obtained as

$$\boldsymbol{\rho}_t = \xi_0 \lambda_0^t \boldsymbol{e}_0 + \xi_1 \lambda_1^t \boldsymbol{e}_1 +, \cdots, +\xi_N \lambda_N^t \boldsymbol{e}_N. \tag{10}$$

Here, the coefficient vector $\boldsymbol{\xi} \stackrel{\mathrm{def}}{=} (\xi_0, \cdots, \xi_N)^{\mathrm{T}}$ is obtained for a given $\boldsymbol{\rho}_0$ as

$$\boldsymbol{\xi} = M^{-1} \boldsymbol{\rho}_0, \tag{11}$$

using principal axis matrix $M \stackrel{\mathrm{def}}{=} [\boldsymbol{e}_0, \cdots, \boldsymbol{e}_N]$, and $\boldsymbol{\rho}_0$ is obtained from its definition ($\boldsymbol{\rho} \stackrel{\mathrm{def}}{=} E(\boldsymbol{\psi}(\boldsymbol{s}))$ using given initial pdf $p_0(\boldsymbol{s})$.

From Assumption 2, $\lambda_0 =, \cdots, = \lambda_{i_1} = 1$. The infinite-time average of Eq. (10) thus converges to

$$\langle \boldsymbol{\rho}_\infty \rangle = \xi_0 \boldsymbol{e}_0 +, \cdots, +\xi_{i_1} \boldsymbol{e}_{i_1}. \tag{12}$$

Therefore, $\langle \boldsymbol{\rho}_\infty \rangle$ is derived as in Eq. (6) using initial pdf $p_0(\boldsymbol{s})$ and $\boldsymbol{e}_0, \cdots, \boldsymbol{e}_{i_1}$ to compute the average pdf in a steady state.

Therefore, the eigenvalues and eigenvectors can be used to find the various properties that cannot be found using conventional analysis methods [12], [13] from the viewpoint of system structure.

3. Low-dimensional Space Embedded Equation Based on Discrete Space Embedding

The space embedded equation (SEE) was developed for expressing an arbitrary multi-dimensional target system as a low-dimensional equation to solve the curse of dimensionality. In this section, the SEE is presented, and the pdf of the target system is derived using the MVE of the SEE.

3.1 Embedding from Multi-dimensional Discrete Space to Low-dimensional Discrete Space

Let $\boldsymbol{\mu} \stackrel{\mathrm{def}}{=} (\mu_1, \cdots, \mu_{d_\mu})^{\mathrm{T}} \in \boldsymbol{\mathcal{D}_\mu}$ be a state vector in a d_μ-dimensional discrete space, $\mu_d \in D_\mu$, $D_\mu \stackrel{\mathrm{def}}{=} \{0, 1, 2, \cdots, 2^B - 1\}$, $\boldsymbol{\mathcal{D}_\mu} \stackrel{\mathrm{def}}{=} D_\mu \times, \cdots, \times D_\mu$, and B be the bit length when μ_d is expressed as a binary number. Let $\sigma \in D_\sigma$ be a state variable in a one-dimensional discrete space, $D_\sigma \stackrel{\mathrm{def}}{=} \{0, 1, 2, \cdots, 2^{d_\mu B} - 1\}$.

First, a mapping from the d_μ-dimensional discrete space to the one-dimensional discrete space, $\tilde{h} : \boldsymbol{\mathcal{D}_\mu} \to D_\sigma$, is defined. Let $b_{d;j} \in \{0, 1\}$ be the jth bit when μ_d is expressed as a binary number, $b_{d;B-1}$ be the most significant bit (MSB), and $b_{d;0}$ be the least significant bit (LSB). Then, μ_d can be expressed as

$$\mu_d = b_{d;0} 2^0 + b_{d;1} 2^1 + b_{d;2} 2^2 +, \cdots, +b_{d;B-1} 2^{B-1}. \tag{13}$$

Two methods were developed to obtain σ from $b_{d;j}$.

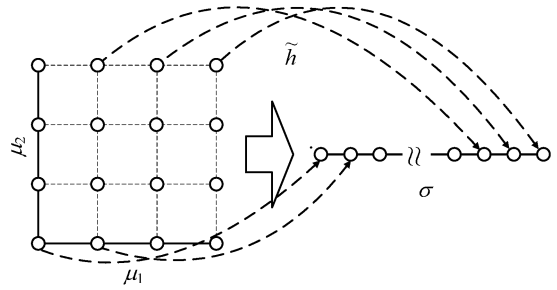

Fig. 1 Mapping $\tilde{h}$ from $\boldsymbol{\mu}$ to σ using PBA.

One is fair bit allocation (FBA), which assigns the significant bits of μ_d for $\forall d$ to those of σ and the less significant bits to those of σ, as described in

$$\begin{aligned}\sigma &= b_{1;0}2^0 + b_{1;1}2^{d_\mu+0} + , \cdots , + b_{1;B-1}2^{(B-1)d_\mu+0} \\ &+ b_{2;0}2^1 + b_{2;1}2^{d_\mu+1} + , \cdots , + b_{2;B-1}2^{(B-1)d_\mu+1} \\ &\quad \vdots \\ &+ b_{d_\mu;0}2^{d_\mu-1} + b_{d_\mu;1}2^{d_\mu+d_\mu-1} + , \cdots , \\ &\qquad + b_{d_\mu;B-1}2^{(B-1)d_\mu+d_\mu-1}.\end{aligned} \tag{14}$$

The other is prior bit allocation (PBA), which assigns the bits of μ_d to the significant bits of σ in the order $\mu_{\theta(d_\mu)}$, $\mu_{\theta(d_\mu-1)}$, $\cdots$, $\mu_{\theta(1)}$. Here, $\theta(d) \in \{1, 2, \cdots, d_\mu\}$ denotes a priority level, and the $\theta(d)$th element of $\boldsymbol{\mu}$ has a dth priority level. That is, $\mu_{\theta(1)}$ has the lowest priority level, and $\mu_{\theta(d_\mu)}$ has the highest priority level. The PBA is defined as

$$\begin{aligned}\sigma &= b_{\theta(1);0}2^0 + b_{\theta(2);0}2^{B+0} + , \cdots , + b_{\theta(d_\mu);0}2^{(d_\mu-1)B+0} \\ &+ b_{\theta(1);1}2^1 + b_{\theta(2);1}2^{B+1} + , \cdots , + b_{\theta(d_\mu);1}2^{(d_\mu-1)B+1} \\ &\quad \vdots \\ &+ b_{\theta(1);B-1}2^{B-1} + b_{\theta(2);B-1}2^{B+B-1} + , \cdots , \\ &\qquad + b_{\theta(d_\mu);B-1}2^{(d_\mu-1)B+B-1}.\end{aligned} \tag{15}$$

The number of values that $\boldsymbol{\mu}$ takes in $\boldsymbol{\mathcal{D}}_{\boldsymbol{\mu}}$ is equal to the number of values that σ takes in D_σ. If $\boldsymbol{\mu} \neq \boldsymbol{\mu}'$, $\tilde{h}(\boldsymbol{\mu}) \neq \tilde{h}(\boldsymbol{\mu}')$ for $\forall \boldsymbol{\mu}$ and $\forall \boldsymbol{\mu}' \in \boldsymbol{\mathcal{D}}_{\boldsymbol{\mu}}$. Thus, $\tilde{h}$ is a bijection and is an embedding[†] from $\boldsymbol{\mathcal{D}}_{\boldsymbol{\mu}}$ to one-dimensional discrete space. An example of $\tilde{h}$ that maps a two-dimensional discrete variable, $\boldsymbol{\mu}$, to a one-dimensional discrete variable, σ, is shown in Fig. 1. Here, μ_2 has the highest priority level.

Mapping $\tilde{h}$ is used to define a mapping from a d_{x}-dimensional discrete variable to a d_{s}-dimensional discrete variable. Let $\tilde{\boldsymbol{x}} \stackrel{\mathrm{def}}{=} (\tilde{x}_1, \cdots, \tilde{x}_{d_{\mathrm{x}}})^{\mathrm{T}}$, $\tilde{x}_d \in \{0, 1, 2, \cdots, 2^B - 1\}$, $\tilde{\boldsymbol{s}} \stackrel{\mathrm{def}}{=} (\tilde{s}_1, \cdots, \tilde{s}_{d_{\mathrm{s}}})^{\mathrm{T}}$, $\tilde{s}_d \in \{0, 1, 2, \cdots, 2^{d_\mu B} - 1\}$, $d_{\mathrm{s}} < d_{\mathrm{x}}$, $mod(d_{\mathrm{x}}, d_{\mathrm{s}}) = 0$, and $d_\mu \stackrel{\mathrm{def}}{=} d_{\mathrm{x}}/d_{\mathrm{s}}$. Here, $mod(d_{\mathrm{x}}, d_{\mathrm{s}})$ is the remainder of division of d_{x} by d_{s}. Then, $\tilde{s}_i$ is obtained as $\tilde{s}_i = \tilde{h}((\tilde{x}_{(i-1)d_\mu+1}, \cdots, \tilde{x}_{id_\mu})^{\mathrm{T}})$. The mapping, $\tilde{\boldsymbol{h}} : \tilde{\boldsymbol{x}} \to \tilde{\boldsymbol{s}}$, is thus a bijection and is described as

$$\begin{aligned}\tilde{\boldsymbol{s}} &= \tilde{\boldsymbol{h}}(\tilde{\boldsymbol{x}}) \\ &\stackrel{\mathrm{def}}{=} (\tilde{h}((\tilde{x}_1, \cdots, \tilde{x}_{d_\mu})^{\mathrm{T}}), \tilde{h}((\tilde{x}_{d_\mu+1}, \cdots, \tilde{x}_{2d_\mu})^{\mathrm{T}}), \cdots , \\ &\qquad \tilde{h}((\tilde{x}_{(d_{\mathrm{s}}-1)d_\mu+1}, \cdots, \tilde{x}_{d_{\mathrm{s}}d_\mu})^{\mathrm{T}}))^{\mathrm{T}}.\end{aligned} \tag{16}$$

[†]The embedding used in this paper is a theoretical concept related to a topological space [16].

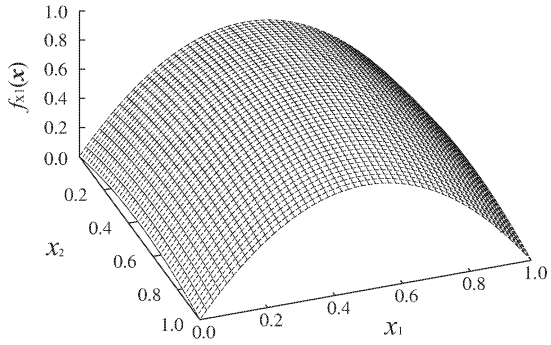

Fig. 2 2D-GCM $f_{\mathrm{x1}}(\boldsymbol{x})$.

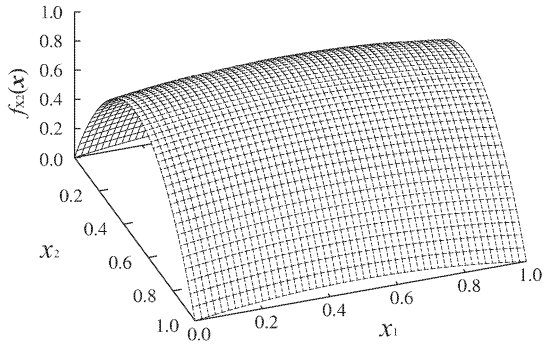

Fig. 3 2D-GCM $f_{\mathrm{x2}}(\boldsymbol{x})$.

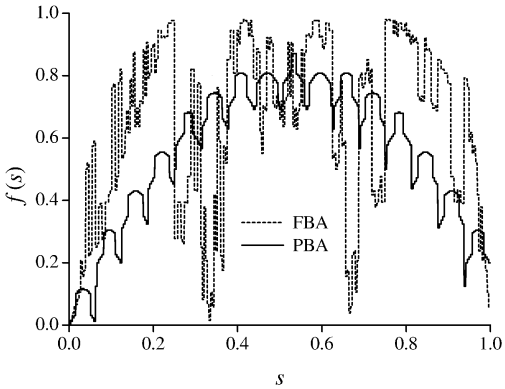

Fig. 4 One-dimensional SEEs of 2D-GCM.

3.2 Low-dimensional Space Embedded Equation of Continuous Multi-dimensional System

Let $\boldsymbol{x} \stackrel{\text{def}}{=} (x_1, \cdots, x_{d_\text{x}})^\text{T} \in \boldsymbol{\mathcal{D}}_\mathbf{x}$ be the d_x-dimensional continuous state, $\boldsymbol{\mathcal{D}}_\mathbf{x} \stackrel{\text{def}}{=} \{\boldsymbol{x} | x_{\min d} \leq x_d \leq x_{\max d}, 1 \leq d \leq d_\text{x}\}$, $\boldsymbol{s} \stackrel{\text{def}}{=} (s_1, \cdots, s_{d_\text{s}})^\text{T} \in \boldsymbol{\mathcal{D}}_\mathbf{s}$ be the d_s-dimensional continuous state, $\boldsymbol{\mathcal{D}}_\mathbf{s} \stackrel{\text{def}}{=} \{\boldsymbol{s} | s_{\min d} \leq s_d \leq s_{\max d}, 1 \leq d \leq d_\text{s}\}$, $d_\text{s} < d_\text{x}$, and $mod(d_\text{x}, d_\text{s}) = 0$.

Mapping $\boldsymbol{h} : \boldsymbol{\mathcal{D}}_\mathbf{x} \rightarrow \boldsymbol{\mathcal{D}}_\mathbf{s}$ maps state $\boldsymbol{x}$ in a multi-dimensional continuous space to state $\boldsymbol{s}$ in a low-dimensional continuous space and is defined as $\boldsymbol{h}(\boldsymbol{x}) \stackrel{\text{def}}{=} \boldsymbol{\Xi}_\text{s}^{-1}(\tilde{\boldsymbol{h}}(\boldsymbol{\Xi}_\text{x}(\boldsymbol{x})))$. Here, $\boldsymbol{\Xi}_\text{x} : \boldsymbol{x} \rightarrow \tilde{\boldsymbol{x}}$ is a mapping from $\boldsymbol{x}$ to discrete state $\tilde{\boldsymbol{x}}$, and $\boldsymbol{\Xi}_\text{s} : \boldsymbol{s} \rightarrow \tilde{\boldsymbol{s}}$ is a mapping from $\boldsymbol{s}$ to discrete state $\tilde{\boldsymbol{s}}$. State $\boldsymbol{s}$ is thus expressed as

$$\boldsymbol{s} = \boldsymbol{h}(\boldsymbol{x}). \tag{17}$$

Let the target multi-dimensional system be

$$\boldsymbol{x}_{t+1} = \boldsymbol{f}_\text{x}(\boldsymbol{x}_t). \tag{18}$$

Using Eq. (17), we can transform the target system into a low-dimensional SEE described by

$$\begin{aligned} \boldsymbol{s}_{t+1} &= \boldsymbol{f}(\boldsymbol{s}_t) \\ &\stackrel{\text{def}}{=} \boldsymbol{h}(\boldsymbol{f}_\text{x}(\boldsymbol{h}^{-1}(\boldsymbol{s}_t))). \end{aligned} \tag{19}$$

Consider the case in which $d_\text{x} = 6$, $d_\text{s} = 2$, and $\theta(3) = 2$ for example. In this case, s_1 represents x_1, x_2, and x_3, and s_2 represents x_4, x_5, and x_6. The variables with the highest priority level are x_2 and x_5, and their dynamics are mainly reflected on those in s_1 and s_2, respectively. Consider the two-dimensional globally coupled logistic map (2D-GCM) defined in Sect. 4.1 as an another example. The elements of the function are shown in Figs. 2 and 3. The one-dimensional SEEs of the two-dimensional coupled logistic map derived using PBA and FBA are shown in Fig. 4. PBA gave the highest priority level to x_1, so x_2 is embedded in x_1, as shown in the figure.

3.3 Pdf of Multi-dimensional State Based on Low-dimensional Space Embedded Equation

The pdf of the target multi-dimensional system in Eq. (18) can be derived using the SEE in Eq. (19). Let Eq. (5) be the MVE of Eq. (19) and the infinite-time average of $\boldsymbol{\rho}_t$ be expressed by Eq. (6). Applying Eq. (17) to Eq. (9), we obtain

$$p(\boldsymbol{x}) = \langle \boldsymbol{\rho}_\infty \rangle^\text{T} \boldsymbol{\psi}^*(\boldsymbol{h}(\boldsymbol{x})). \tag{20}$$

The algorithm for deriving the pdf is summarized as Algorithm 1.

Algorithm 1: Analysis based on MVE of SEE

(1-1) Set target system in Eq. (18) and derive its SEE in Eq. (19).

(1-2) Compute matrix A in MVE of Eq. (19).

(1-3) Compute eigenvalues and eigenvectors of matrix A.

(1-4) If there are multiple eigenvalues with value 1, set weight w_i used for Eq. (6).

(1-5) Compute $\langle \boldsymbol{\rho}_\infty \rangle$ using Eq. (6), and compute pdf using $\langle \boldsymbol{\rho}_\infty \rangle$ and Eq. (20).

(1-6) Change weight w_i and go back to Step (1-5) if necessary.

Hereinafter, the MVE of an SEE that uses PBA is abbreviated as MVE(PBA). When FBA is used instead of PBA, it is abbreviated as MVE(FBA). When the SEE is not used, that is, $d_\text{x} = d_\text{s}$ and $\boldsymbol{s} = \boldsymbol{h}(\boldsymbol{x}) = \boldsymbol{x}$, the MVE is referred to as MVE(original).

When MVE(PBA) is used, the dynamics in the variable with the highest priority level in $x_{(i-1)d_\mu+1}, \cdots, x_{id_\mu}$ are reflected on those in s_i. The degree of expansion, N, is thus derived using Eq. (A·6) as

$$N = \begin{cases} \displaystyle\prod_{d=1}^{d_\text{x}} (N_d + 1) - 1 \ \text{ for MVE(original)} \\ \displaystyle\prod_{d=1}^{d_\text{s}} (N_d + 1) - 1 \ \text{ for MVE(PBA).} \end{cases} \tag{21}$$

Dimension reduction using the SEE has an attractive feature: the pdfs of arbitrary elements in the target nonlinear system can be derived without a reduction in accuracy due to dimension reduction. In other words, Eq. (21) means that the degree of expansion can be reduced from N to around $N^{(d_\text{s}/d_\text{x})}$ while maintaining the accuracy of the variable with the highest priority level.

Consider an example in which $d_\text{x} = 4$, $d_\text{s} = 1$, and $\theta(4) = 2$. In this example, s_1 represents x_1, x_2, x_3, and x_4. The variable with the highest priority level is x_2, and its dynamics are mainly reflected on those in s_1. We can thus analyze the dynamics in x_2 in the one-dimensional space of s_1 instead of the four-dimensional space of x_1, $\cdots$, x_4. When $N_d = 32$ for $\forall d$, that is, all the x_d have the same accuracy, the N of MVE(PBA) is 32 whereas that of MVE(original) is 1,185,920. It is thus difficult to use MVE(original) for systems with more than four dimensions. Thus, MVE(PBA) can be used to analyze a target system that cannot be analyzed using MVE(original), and we can obtain pdfs for all the x_d and their joint pdf by executing Algorithm 1 for various combinations of $\theta(d)$. In contrast, the bits of x_1,$\cdots$, x_{d_x} are fairly assigned to s_1,$\cdots$, s_{d_s} in MVE(FBA). The accuracies for each state are thus much lower than those obtained using MVE(PBA). These properties of MVE(FBA) and MVE(PBA) are evaluated in the next section.

4. Performance Evaluation

4.1 Effect of Degree of Expansion on Accuracy

Consider a globally coupled map (GCM) [17] as the target system in Eq. (18). The GCM is defined by

$$\begin{aligned} \boldsymbol{x}_{t+1} &= \boldsymbol{f}_{\mathrm{x}}(\boldsymbol{x}_t) \\ &\stackrel{\mathrm{def}}{=} C\boldsymbol{g}^{(n)}(\boldsymbol{x}_t), \end{aligned} \tag{22}$$

where $\boldsymbol{g}^{(n)}(\boldsymbol{x}) \stackrel{\mathrm{def}}{=} (g_1^{(n)}(x_1), \cdots, g_{d_{\mathrm{x}}}^{(n)}(x_{d_{\mathrm{x}}}))^{\mathrm{T}}$, $g_i^{(n)}(x) \stackrel{\mathrm{def}}{=} \overbrace{g_i(g_i(\cdots g_i(x)\cdots))}^{n}$, $g_i(x)$ is a logistic map defined by $g_i(x_i) \stackrel{\mathrm{def}}{=} a_i x_i(1-x_i)$ [18], and C is a $d_{\mathrm{x}} \times d_{\mathrm{x}}$ matrix.

In this section, the effectiveness of MVE(PBA) for the dimension reduction described in Sect. 3.3 is evaluated. It is shown that the degree of expansion can be reduced from N to around $N^{(d_{\mathrm{s}}/d_{\mathrm{x}})}$ by using MVE(PBA) and that the accuracy of the pdf of the variable with the highest priority level does not decrease due to dimension reduction. Consider a two-dimensional GCM (2D-GCM) with parameters $n = 1$, $d_{\mathrm{x}} = 2$, $a_1 = 3.2$, $a_2 = 3.9$, and $C = C_1$, where C_1 is given by

$$C_1 \stackrel{\mathrm{def}}{=} \begin{bmatrix} 0.9 & 0.1 \\ 0.1 & 0.9 \end{bmatrix}.$$

The x_1 oscillates periodically with a period of 2 when x_1 and x_2 behave independently (i.e., C is an identity matrix). In contrast, both x_1 and x_2 for $C = C_1$ show chaotic dynamics because the strong nonlinearity in x_2 with chaotic dynamics affects x_1, as can be seen in their pdfs in Fig. 5. It is thus difficult to analyze the GCM using conventional methods, which decompose it into elements and then combine their properties. Therefore, the GCM is used to evaluate the performance of the method described in Sect. 3.

First, the effect of N, the degree of expansion, on the pdf of 2D-GCM was evaluated to show that the accuracy of the pdf increases with N. Figure 6 shows the effect of N on the pdfs of x_1 and x_2 obtained using MVE(PBA) with $d_{\mathrm{s}} = 1$. It is obvious, comparing Figs. 5 and 6, that the accuracy increased with N.

Second, the accuracy of the pdf of the variable with the highest priority level was shown not to decrease due to dimension reduction. Figure 7 shows the effect of N on the pdf when MVE(original) was used. The accuracy of the pdf obtained using MVE(original) with $N = 255$ was almost equal to that obtained using MVE(PBA) with $N = 15$, as we can see by comparing Figs. 6 and 7. This means that we can reduce the degree of expansion from N to around $N^{(d_{\mathrm{s}}/d_{\mathrm{x}})}$ ($d_{\mathrm{s}} = 1$ and $d_{\mathrm{x}} = 2$) using MVE(PBA) without a reduction in accuracy of the pdf due to dimension reduction.

To identify the reason for this, the pdfs obtained using MVE(PBA) and MVE(FBA) for $N = 15$ and

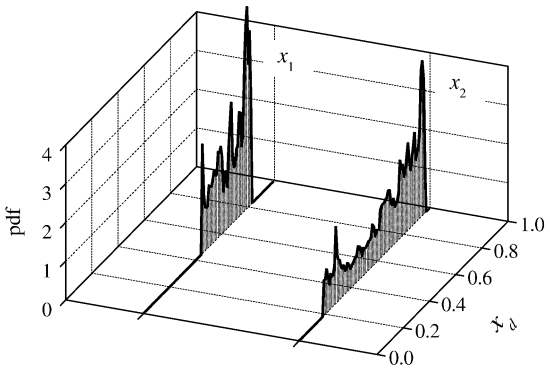

Fig. 5 Pdfs of 2D-GCM obtained using numerical simulation.

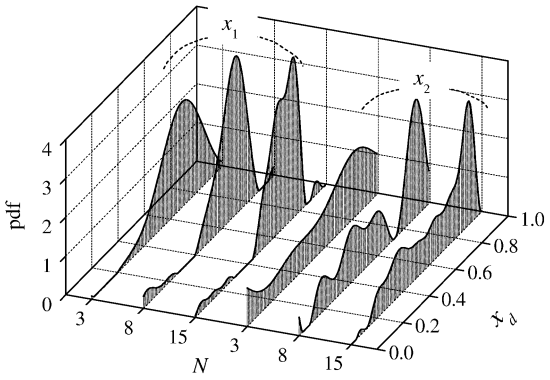

Fig. 6 Pdfs of 2D-GCM obtained using MVE(PBA).

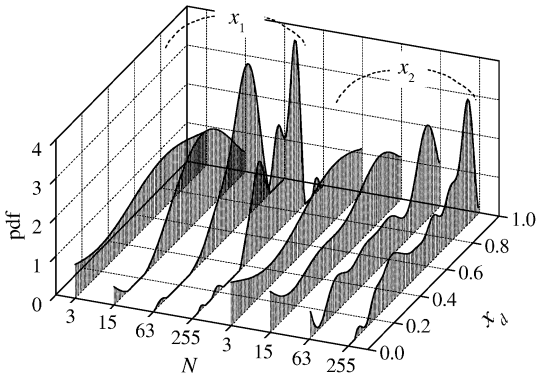

Fig. 7 Pdfs of 2D-GCM obtained using MVE(original).

$d_{\mathrm{s}} = 1$ are plotted in Fig. 8, where all the pdfs obtained using MVE(PBA) are shown while only the pdfs of $x_{\theta(2)}$ (the state with the highest priority level) are shown in Fig. 6. When MVE(PBA) with $\theta(1) = 2$ and $\theta(2) = 1$ was used, the dynamics in x_1 were mainly reflected on those in s_1. The accuracy for s_1 was thus substantially proportional to N, and that for x_2 was almost equal to 0. This is illustrated by the plot in Fig. 8, where the pdf of x_1 is similar to that obtained using MVE(original) with $N = 255$, as in Fig. 7, al-

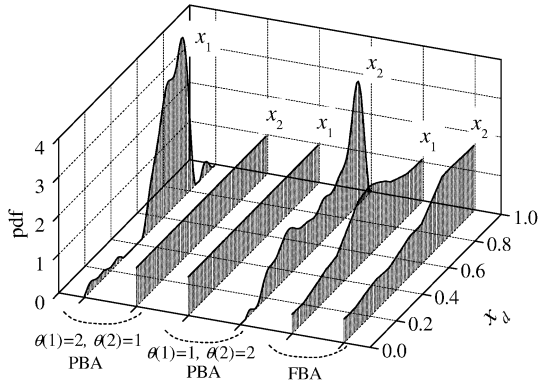

Fig. 8 Pdfs of 2D-GCM obtained using MVE(PBA) and MVE(FBA) (N=15).

though the pdf of x_2 cannot express the dynamics in x_2. When MVE(PBA) with $\theta(1) = 1$ and $\theta(2) = 2$ was used, the pdf of x_2 expressed an approximate pdf for the same reason. These results show that we can select an arbitrary element in state $\boldsymbol{x}$ and derive the properties of that element without degrading its accuracy at the expense of the accuracies of the other elements. In contrast, when MVE(FBA) was used, the dynamics in both x_1 and x_2 were reflected on those in s_1. The accuracy was thus worse than that of MVE(PBA).

In short, the degree of expansion can be reduced from N to around $N^{(d_{\rm s}/d_{\rm x})}$ by using MVE(PBA), and the accuracy of the pdf of the variable with the highest priority level is not reduced due to dimension reduction. Therefore, MVE(PBA) is suitable for analyzing multi-dimensional systems although we have to repeatedly execute Algorithm 1 for various combinations of $\theta(d)$.

4.2 Multiple Attractors

The 2D-GCM described in the previous section has a unique attractor. In contrast, there are many systems in which states starting from different initial values depict different attractors. Multiple attractors can be derived from MVE(PBA). Consider a four-dimensional GCM (4D-GCM) with parameters $n = 2$, $d_{\rm x} = 4$, $a_1 = 3.65$, $a_2 = 3.7$, $a_3 = 3.55$, $a_4 = 3.6$, and $C = C_2$ given by

$$C_2 \stackrel{\rm def}{=} \begin{bmatrix} 0.9 & 0.1 & 0 & 0 \\ 0 & 0.9 & 0.1 & 0 \\ 0 & 0 & 0.9 & 0.1 \\ 0.1 & 0 & 0 & 0.9 \end{bmatrix}.$$

The parameters were set so that the GCM clearly provided multiple attractors with different pdfs due to the initial value of $\boldsymbol{x}_t$ to confirm that eigen analysis of the MVE can identify multiple steady states.

The pdfs of x_1 obtained using numerical simulation are shown in Fig. 9 (labeled "Attractor 1" and "Attractor 2"). Fortunately, multiple attractors for the 4D-GCM were obtained by numerical simulation for different initial values of $\boldsymbol{x}$, as shown in Fig. 9, although it is often difficult to obtain multiple attractors by numerical simulations [13]. However, it is still difficult to determine how many kinds of attractors the system can provide. Moreover, MVE(original) cannot be used for systems with more than four dimensions, as discussed in Sect. 3.3, because N becomes too large. Eigen analysis of matrix A of the MVE of the SEE is thus a powerful way to find multiple attractors for systems with more than four dimensions even if they are difficult to find using numerical simulation [13].

Table 1 Eigenvalues for 2D-GCM and 4D-GCM.

	2D-GCM		4D-GCM	
i	λ_i	$\lvert\lambda_i\rvert$	λ_i	$\lvert\lambda_i\rvert$
0	$1.00 + 0.00\imath$	1.00	$1.00 + 0.00\imath$	1.00
1	$-0.90 + 0.00\imath$	0.90	$1.00 + 0.00\imath$	1.00
2	$0.01 + 0.51\imath$	0.51	$-0.60 + 0.00\imath$	0.60
3	$0.02 - 0.47\imath$	0.47	$0.27 + 0.07\imath$	0.28

Set $d_{\rm s} = 1$ and the highest priority to x_1 to investigate the attractors of x_1. As shown in Table 1, λ_0 and λ_1 take unity, where $\imath$ denotes the imaginary unit. This means that there are two types of pdfs with respect to x_1 and that the shape of the average pdf in a steady state depends on the initial pdf, as obtained using numerical simulation. The pdfs for $N = 32$ are shown in Fig. 10, and they are sufficiently precise to discriminate the differences between them.

The w_1 in Eq. (6) is determined so that $p(\boldsymbol{x})$ in Eq. (20) is not less than zero for $\forall \boldsymbol{x} \in \boldsymbol{\mathcal{D}}_{\mathbf{x}}$. For 4D-GCM, $p(\boldsymbol{x}) \geq 0$ for $-4.0 \leq w_1 \leq -0.5$, and $p(\boldsymbol{x})$ with $w_1 = -0.5$ shows Attractor 1 and that with -4.0 shows Attractor 2. When $-4.0 < w_1 < -0.5$, the pdf is a mixture of the pdfs of Attractors 1 and 2, and it is obtained when there are multiple particles that obey 4D-GCM independently. The value of w_1 corresponds to the ratio of the number of particles that obey Attractor 1 or 2. An example pdf for multiple particles is shown in Figs. 9 and 10 (indicated by "Mixture"). In the same manner as for 4D-GCM, consider the eigenvalues of 2D-GCM shown in Table 1. Only λ_0 takes unity. This means that $\langle \boldsymbol{\rho}_\infty \rangle$ has a unique value, as in Eq. (6). The average pdf in a steady state should thus be unique. This was confirmed by numerical simulation using various initial values of x_0. These results show that the number of attractors and their pdfs that a system provides can be estimated using eigen analysis of matrix A.

5. Conclusion

The space embedded equation (SEE) presented in this paper can be used to express a multi-dimensional target system as a low-dimensional equation. The problem of the dimension of the moment vector equation (MVE) increasing geometrically with the dimension of the target system can be avoided by using the SEE without

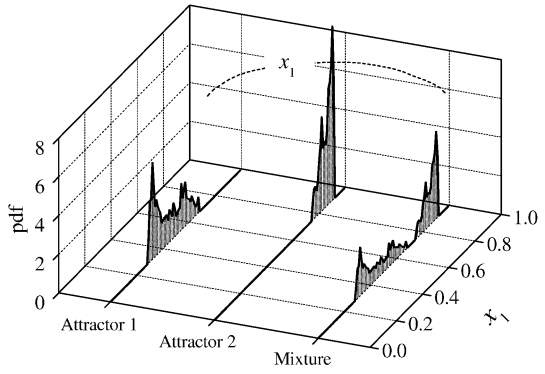

Fig. 9 Pdfs of 4D-GCM obtained using numerical simulation.

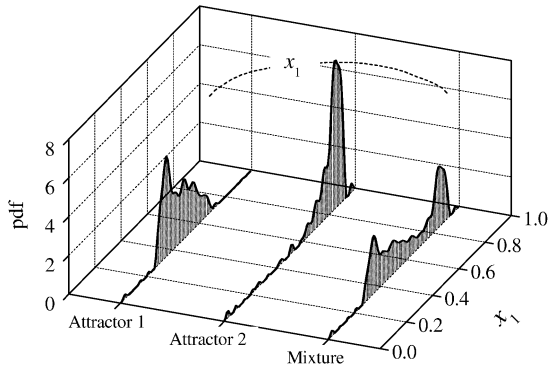

Fig. 10 Pdfs of 4D-GCM obtained using MVE(PBA).

a reduction in accuracy due to dimension reduction. Eigen analysis of the MVE is effective for identifying the macroscopic and statistical properties that cannot be identified using numerical simulation. Therefore, the MVE using SEE approach can be applied to multi-dimensional nonlinear systems to find various properties that cannot otherwise be found. It is difficult to analyze a very-high-dimensional system using the MVE of the SEE presented in this paper. This is because the accuracy of the pdf cannot be maintained due to the quantization (discretization) errors in mapping Ξ and $\tilde{h}$ without increasing calculation time. In other words, it takes a very long time to derive MVE(PBA) if we try to maintain the accuracy for a very-high-dimensional system. Fortunately, it is possible to reduce the errors and improve the accuracy of MVE of SEE by using ultradiscretization [19] and the Markov partition [20]. Although applying these methods is a challenging task, they are quite promising for improving the accuracy because of their attractive features, so this challenge will be taken up in a future study.

References

[1] B. Scholkopf, A. Smola, and K. R. Muller, "Nonlinear Component Analysis as a Kernel Eigenvalue Problem," Neural Computation vol. 10, no. 5, pp. 1299–1319, 1998.

[2] J. B. Tenenbaum, V. Silva, and J. C. Langford, "A Global Geometric Framework for Nonlinear Dimensionality Reduction," Science 22, vol. 290, no. 5500, pp. 2319–2323, Dec. 2000.

[3] I. Menache, S. Mannor, and N.Shimkin, "Basis function adaptation in temporal difference reinforcement learning," Annals of Operations Research, vol. 134, no. 1, pp. 215–238, Feb. 2005.

[4] S. Mahadevan and M. Maggioni, "Value function approximation using diffusion wavelets and Laplacian eigenfunctions," Neural Information Processing Systems (NIPS) MIT Press, 2006.

[5] J. Johns and S. Mahadevan, "Constructing basis functions from directed graphs for value function approximation," Proceedings of the 24th international conference on Machine learning, pp. 385–392, 2007.

[6] J. Teramae and D. Tanaka, "Robustness of the noise-induced phase synchronization in a general class of limit cycle oscillators," Phys. Rev. Lett. vol. 93, no. 20, 204103 pp. 1–4, Nov. 2004.

[7] G. L. Oppo and A. Politi, "Center-manifold reduction for laser equations with detuning," Phys. Rev. A, vol. 40, no. 3, pp. 1422–1427, Aug. 1989.

[8] A. F. Vakakis and M. E. King, "Resonant oscillations of a weakly coupled nonlinear layered system," Acta Mech., vol. 128, no. 1-2, pp. 59-80, 1998.

[9] K. Komatsu and H. Takata, "A Formal Linearization by the Chebyshev Interpolation and Its Applications", Proceedings of the IEEE Conference on Decision and Control, vol. 1 of 4, pp.70–75, 1996.

[10] T. Kohda and K. Murao, "Approach to Time Series Analysis for One-Dimensional Chaos Based on Frobenius-Perron Operator," IEICE Transactions, vol. E73-E, no. 6, pp. 793–800, June 1990.

[11] L. Billings and I. B. Schwartz, "Identifying almost invariant sets in stochastic dynamical systems," Chaos, vol. 18, no. 2, pp. 023122-1–8, June 2008.

[12] H. Satoh, "Approximation and analysis of non-linear equations in a moment vector space," IEICE Trans. Fundamentals, vol. E89-A, no. 1, pp. 270–279, Jan. 2006.

[13] H. Satoh, "Analysis based on moment vector equation for interacting identical elements with nonlinear dynamics," IEICE Trans. Fundamentals, vol. E93-A, no. 10, pp. 1765–1774, Oct. 2010.

[14] D. Jiulin, "The nonextensive parameter and Tsallis distribution for self-gravitating systems," Europhys. Lett., vol. 67, no. 6, pp. 893–899, Sept. 2004.

[15] T. D. Frank, "Short-time correlations of many-body systems described by nonlinear Fokker-Planck equations and Vlasov-Fokker-Planck equations," Physics Letters A, vol. 337, no. 3, pp. 224–234, April 2005.

[16] S. Lipschutz, Schaum's Outline Series Theory and Problems of General Topology, McGraw-Hill, USA, 1964.

[17] K. Kaneko, "Clustering coding switching hierarchical ordering and control in a network of chaotic elements," Physica D, vol. 41, pp. 137–172, 1990.

[18] E. Ott, Chaos in Dynamical Systems Second ed., Cambridge University Press, UK, 2002.

[19] D. Takahashi, T. Tokihiro, B. Grammaticos, Y. Ohta, and A. Ramani, "Constructing solutions to the ultradiscrete Painleve equations," J. Phys. A: Math. Gen., vol. 30, no. 22, pp. 7953–7966, 1997.

[20] C. Robinson, Dynamical Systems: Stability Symbolic Dynamics and Chaos 2nd Ed., CRC Press, Yew York, 1999.

Appendix A: Basis for Function Approximation

An orthonormal basis is summarized in this appendix. Let $h(\boldsymbol{k})$ be the Fourier coefficient, $\boldsymbol{k} \stackrel{\text{def}}{=} (k_1, \cdots, k_{d_\text{s}})^\text{T} \in \boldsymbol{\mathcal{Z}}$ be the index vector of the Fourier coefficient, and $\boldsymbol{\mathcal{Z}}$ be the set of $\boldsymbol{k}$ that are used for the index vectors. The Fourier series expansion for function $f(\boldsymbol{s})$ is defined by

$$f(\boldsymbol{s}) = \sum_{\boldsymbol{k} \in \boldsymbol{Z}} h(\boldsymbol{k}) K(\boldsymbol{s}, \boldsymbol{k}), \tag{A·1}$$

$$h(\boldsymbol{k}) \stackrel{\text{def}}{=} \int_{\boldsymbol{\mathcal{D}_\text{s}}} f(\boldsymbol{s}) K^*(\boldsymbol{s}, \boldsymbol{k}) \text{d}\boldsymbol{s}, \tag{A·2}$$

where $\boldsymbol{s} \stackrel{\text{def}}{=} (s_1, \cdots, s_{d_\text{s}})^\text{T}$ is the state vector of dimension d_s, $\boldsymbol{\mathcal{D}_\text{s}} \stackrel{\text{def}}{=} \{\boldsymbol{s} | s_{\min d} \leq s_d \leq s_{\max d}, 1 \leq d \leq d_\text{s}\}$ is the domain of the definition of $\boldsymbol{s}$, superscript $*$ denotes a complex conjugate, $\{K(\boldsymbol{s}, \boldsymbol{k})\}$ is a multi-dimensional orthonormal basis, and K($\boldsymbol{s}$,$\boldsymbol{k}$) is defined by

$$K(\boldsymbol{s}, \boldsymbol{k}) \stackrel{\text{def}}{=} \prod_{d=1}^{d_\text{s}} K_d(s_d, k_d). \tag{A·3}$$

Here, $\{K_d(s_d, k_d)\}$ is a one-dimensional orthonormal basis.

Let $\{\psi_i(\cdot)\}$ be a basis the element of which is defined by

$$\psi_i(\boldsymbol{s}) \stackrel{\text{def}}{=} K(\boldsymbol{s}, \boldsymbol{k}), \tag{A·4}$$

where i is the index of the basis. When $\mathcal{Z}_d \stackrel{\text{def}}{=} \{0, 1, \cdots, N_d\}$ and $\boldsymbol{\mathcal{Z}}$ is given by the Cartesian product as $\boldsymbol{\mathcal{Z}} = \mathcal{Z}_1 \times \mathcal{Z}_2 \times, \cdots, \times \mathcal{Z}_{d_\text{s}}$, the relationship between $\boldsymbol{k}$ and i can be obtained using

$$i = \sum_{d=1}^{d_\text{s}} k_d \prod_{d'=d+1}^{d_\text{s}} (N_{d'} + 1), \tag{A·5}$$

where N_d is the degree of expansion of s_d. Let N be the degree of expansion of $\boldsymbol{s}$. When Eq. (A·5) holds, N is expressed by

$$N = \prod_{d=1}^{d_\text{s}} (N_d + 1) - 1, \tag{A·6}$$

where the dimension of the feature space with the basis is $N + 1$. The relationship between i and $\boldsymbol{k}$ is referred to as the index table.

The element of the orthonormal basis based on the complex Fourier series is defined as

$$K_d(s_d, k_d) \stackrel{\text{def}}{=}$$
$$\begin{cases} \sqrt{\dfrac{1}{D_{\text{s}d}}} & \text{for } k_d = 0 \\ \sqrt{\dfrac{1}{D_{\text{s}d}}} \exp(-\imath \dfrac{k_d+1}{2} \omega_{0d} (s_d - s_{\min d})) & \text{for } k_d = 1, 3, \cdots \\ \sqrt{\dfrac{1}{D_{\text{s}d}}} \exp(\imath \dfrac{k_d}{2} \omega_{0d} (s_d - s_{\min d})) & \text{for } k_d = 2, 4, \cdots \end{cases}$$

where $\imath$ denotes the imaginary unit, $\omega_{0d} \stackrel{\text{def}}{=} 2\pi / D_{\text{s}d}$, and $D_{\text{s}d} \stackrel{\text{def}}{=} s_{\max d} - s_{\min d}$.

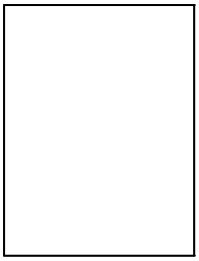

Hideki Satoh Hideki Satoh received B.E. and M.E. degrees in Electronics and Communication Engineering from Waseda University in 1984 and 1987, respectively, and a Ph.D. degree in Information Science from Waseda University in 2002. He joined the Corporate Research & Development Center, Toshiba Corp., in 1987. In 2000, he worked on 4th-generation mobile communication systems at YRP Mobile Telecommunications Key Technology Research Laboratories Co., Ltd. Since 2002, he has been investigating nonlinear science and communication theory at Future University Hakodate.